Fermionic Many-Body Localization for Random and Quasiperiodic Systems in the Presence of Short- and Long-Range Interactions

Vu, DinhDuy; Huang, Ke; Li, Xiao; Das Sarma, Sankar

Published in:
Physical Review Letters

Published: 08/04/2022

Document Version:
Final Published version, also known as Publisher's PDF, Publisher's Final version or Version of Record

Published version (DOI):
10.1103/PhysRevLett.128.146601

Publication details:
Vu, D., Huang, K., Li, X., & Das Sarma, S. (2022). Fermionic Many-Body Localization for Random and Quasiperiodic Systems in the Presence of Short- and Long-Range Interactions. *Physical Review Letters*, *128*(14), Article 146601. Advance online publication. https://doi.org/10.1103/PhysRevLett.128.146601

Vu, D., Huang, K., Li, X., & Das Sarma, S. (2022). Fermionic Many-Body Localization for Random and Quasiperiodic Systems in the Presence of Short- and Long-Range Interactions. *Physical Review Letters, 128*(14), Article 146601. https://doi.org/10.1103/PhysRevLett.128.146601.

Fermionic Many-Body Localization for Random and Quasiperiodic Systems in the Presence of Short- and Long-Range Interactions

DinhDuy Vu,[1] Ke Huang,[2] Xiao Li,[2,3] and S. Das Sarma[1]
[1]Condensed Matter Theory Center and Joint Quantum Institute, University of Maryland, College Park, Maryland 20742, USA
[2]Department of Physics, City University of Hong Kong, Kowloon, Hong Kong SAR
[3]City University of Hong Kong Shenzhen Research Institute, Shenzhen 518057, Guangdong, China

(Received 22 September 2021; revised 6 December 2021; accepted 20 March 2022; published 6 April 2022)

We study many-body localization (MBL) for interacting one-dimensional lattice fermions in random (Anderson) and quasiperiodic (Aubry-Andre) models, focusing on the role of interaction range. We obtain the MBL quantum phase diagrams by calculating the experimentally relevant inverse participation ratio (IPR) at half-filling using exact diagonalization methods and extrapolating to the infinite system size. For short-range interactions, our results produce in the phase diagram a qualitative symmetry between weak and strong interaction limits. For long-range interactions, no such symmetry exists as the strongly interacting system is always many-body localized, independent of the effective disorder strength, and the system is analogous to a pinned Wigner crystal. We obtain various scaling exponents for the IPR, suggesting conditions for different MBL regimes arising from interaction effects.

DOI: 10.1103/PhysRevLett.128.146601

Introduction.—Many-body localization (MBL), an extensively recently studied phenomenon in quantum statistical mechanics [1–4], deals with the important subject of thermalization in isolated disordered interacting quantum systems, where all eigenstates (i.e., the whole many-body spectrum, not just the ground state) may become localized for strong enough disorder even in the presence of interactions, thus preventing the system from achieving equilibrium although interaction among the particles should allow energy transport, in principle.

MBL, which is a generalization of the well-known ground-state Anderson localization [5] to the whole many-body interacting spectrum, is a counterexample to the quantum eigenstate thermalization hypothesis [6,7], and as such, violates the basic premise of quantum statistical mechanics. Little is known about MBL theoretically, as the standard analytical tools of theoretical physics do not quite apply in dealing with the dynamics of interacting disordered systems in the nonequilibrium thermodynamic limit. However, an early work using perturbation theory on a Bethe lattice hinted at the existence of the MBL transition from extended thermal to localized nonthermal situation [8], and a rigorous argument exists for the existence of a localized spectrum (but, not for the MBL transition) in interacting spin chains for sufficiently large disorder [9,10]. Most theoretical works on MBL therefore resort to small-system numerics on one-dimensional lattices, which clearly shows the existence of MBL in both purely random Anderson-type (A) disorder model and quasiperiodic Aubry-Andre-type (AA) quasiperiodic model [11], at least for finite systems [12–17]. In the current work we use exact diagonalization methods to study fermionic MBL in A and AA models, both for short-range (SR) and long-range (LR) interactions. Our physically motivated fermionic long-range interaction is qualitatively different from, but nevertheless can be mapped to an anisotropic spin model with the long-range ZZ coupling. In contrast, the long-range XX and YY components do not have a physical fermionic counterpart because they intrinsically involve long-range hoppings, which are always suppressed exponentially in physical systems. In principle, long-range hopping can cause delocalization as discussed in Refs. [18–24]. This qualitatively distinguishes our study from previous works on spin models [22–25]. We also note that fermionic MBL with long-range interactions has been discussed in the context of Luttinger liquids [26,27] and self-consistent mean field theory [28]. These treatments apply to at most moderate interaction, comparable to the energy scale of the noninteracting counterpart, but not to a very strong interacting regime where the Hilbert space is immensely partitioned. Our study indeed shows that MBL persists longer for long-range interactions with weak to moderate strength, consistent with other theoretical approaches. However, as shown in our phase diagrams (see the $U \leq 5$ regime of Fig. 4), this effect is mostly quantitative compared to the much more apparent interaction-range dependence observed in the strongly interacting regime. This is the key advancement in our work. Finally, MBL has been reported in experimental studies of ultracold atoms on lattices [29–32], where our work applies directly.

In the current work we aim at the ambitious challenge of calculating the MBL quantum phase diagram in the disorder-interaction space for interacting fermions on a (half-filled) 1D lattice, separately considering both short-range

and long-range interparticle interactions. The key new features of our work are (i) the consideration of the whole range of interaction, from weak to strong, in obtaining the MBL phase diagram, and (ii) the consideration of LR interaction (in addition to the SR interaction, used extensively in the existing MBL literature). We find that for strong LR interactions, MBL exists generically in both A and AA models for any disorder, no matter how small the disorder is. For SR interactions, we find an approximate symmetry between MBL properties at very weak and very strong interactions, which arises from the nature of the Hubbard model employed in our work. For weak to modest interaction, SR and LR interactions produce similar results even though, quantitatively, the MBL phase slightly extends for LR interaction. These two cases studied here can help us understand the localization property of a generic interaction case.

Model.—The physical systems in our paper are modeled by the following Hamiltonian of spinless electrons:

$$H = \sum_i [(c_i^\dagger c_{i+1} + \text{H.c.}) + V_i n_i] + \frac{1}{2}\sum_{i,j} U_{i,j} n_i n_j. \tag{1}$$

Here the AA potential is $V_i = V\cos(2\pi i/\beta + \phi)$ with $\beta = (\sqrt{5}+1)/2$ and a random phase ϕ, while for the random A potential, each V_i is picked from a uniform distribution $[-V, V]$. The hopping is limited to nearest sites, reflecting the realistic situation in 1D fermionic systems including both solid state lattices and cold-atom arrays. The effect of electron-electron interaction is studied in two representative cases: the SR nearest-neighbor interaction $U_{i,j} = U\delta_{i\pm1,j}$ and the LR interaction

$$U_{i,j} = U\left(\frac{L}{\pi}\sin\frac{\pi|i-j|}{L}\right)^{-\kappa}. \tag{2}$$

For now we only consider $\kappa = 1$. Together, we present four 2D phase diagrams in the interaction-disorder plane: AA model (SR), AA model (LR), A model (SR), and A model (LR). Our goal is the localization and extension property in the thermodynamic limit. We expect that a qualitative picture can be systematically obtained from finite-size calculations. In particular, for each type of disorder and interaction, we exactly diagonalize finite-size Hamiltonians of different numbers of sites L and electrons N_e (with the filling fraction $\nu = N_e/L$ fixed at $1/2$). The results are then extrapolated to the limit $L \to \infty$, providing predictions about the half-filled system in the thermodynamic limit [18,33,35]. We impose the periodic boundary condition $c_{L+1} = c_1$ to eliminate the boundary effects in finite-size calculations.

After diagonalizing the finite-size Hamiltonian (1), the localization property of each eigenstate ψ_λ (λ is the label of many-body eigenstates) can be quantified by the scaled inverse participation ratio (IPR) [36], defined as

$$\mathcal{I}^{(\lambda)} = \frac{1}{1-\nu}\left(N_e^{-1}\sum_{i=1}^{L}|u_i^{(\lambda)}|^2 - \nu\right), \tag{3}$$

where $u_i^{(\lambda)} \equiv \langle\psi_\lambda|n_i|\psi_\lambda\rangle$ is the projected particle number of each state ψ_λ on site i. In the maximally extended state, $u_i = N_e/L$, resulting in $\mathcal{I} = 0$; while in the opposite limit, $u_i = 1$ (0) for an occupied (vacant) site, corresponding to $\mathcal{I} = 1$. Therefore, a generic eigenstate has $0 \le \mathcal{I} \le 1$. To benchmark the degree of localization of the whole spectrum, we use the infinite-temperature (arithmetic mean) scaled IPR, $\langle\mathcal{I}\rangle \equiv \sum_\lambda \mathcal{I}^{(\lambda)}/d$, with d being the dimension of the Hilbert space. For brevity, we will refer to $\langle\mathcal{I}\rangle$ simply as the mean IPR.

Quantum phase diagram.—By exact diagonalization, we compute the mean IPR as a function of U and V for five different system sizes, $L = 8, \ldots, 16$ at half filling, and extrapolate these results into the limit $N_e \to \infty$ to obtain the phase diagram. The AA model results are averaged over six random phases, while the A model results are averaged over six random disorder realizations. This number of realizations is sufficient for our purpose, as confirmed by our numerical investigation. The calculated MBL phase diagrams are presented in Fig. 1.

It is well established that the noninteracting AA model has a critical point at $V = 2$, with the whole spectrum localized (extended) for $V > 2$ ($V < 2$). By contrast, the A model is always localized for any $V > 0$ [we refer to [33] or Figs. 2(c) and 2(d) for better visibility]. Figure 1 shows that, for both models of interactions, this noninteracting localization persists in the regime $U \ll 1$, consistent with the statement that MBL exists for perturbatively weak interactions [8,28,37]. This might also apply to some cases of

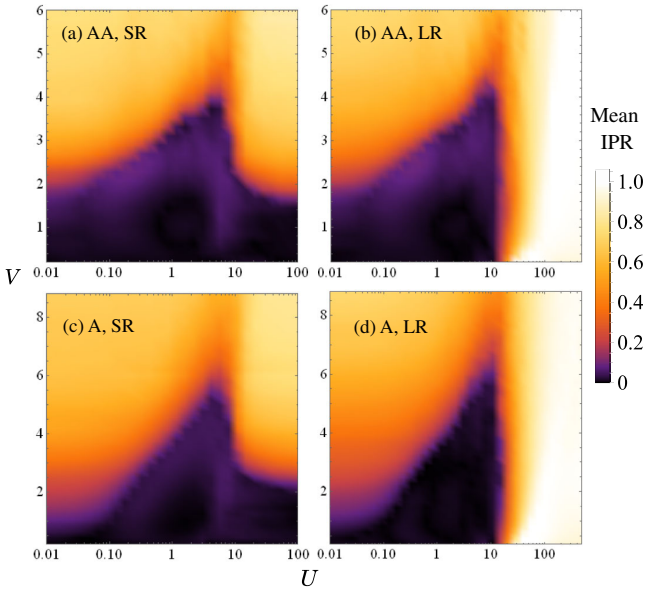

FIG. 1. Extrapolated quantum phase diagram from simulations on finite-size lattices of $L = 8, 10, \ldots, 16$.

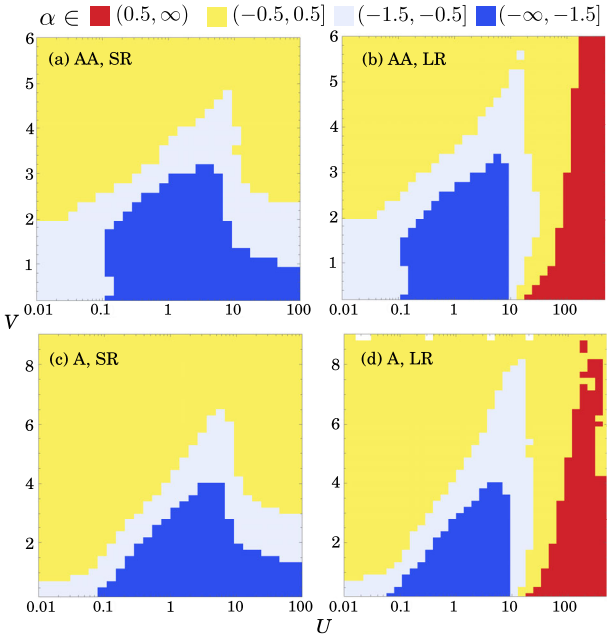

FIG. 2. The effective scaling exponent α is divided into four color-coded regimes: (i) the marginal localized phase $\alpha \approx 0$ (yellow), (ii) the reciprocal extended phase $\alpha \approx -1$ (light blue), (iii) the relevant localized phase $\alpha > 0$ (red), and (iv) the super-reciprocal extended phase $\alpha < -1$ (dark blue).

systems with mobility edge [35]. However, when $U \sim \mathcal{O}(1)$, there exists a transition from the MBL to the thermal phase (as a function of U) that depends highly on the underlying noninteracting model but quantitatively little on the interaction type. Specifically, in the extrapolated thermodynamic limit, the thermal phase extends to $V \sim 4$ for the AA model and $V \sim 6$ for the A model, above which the corresponding interacting phase is always MBL. This transition might be understood from the reordering of Fock state energy levels (disorder plus interaction potential), resulting in level crossings as U increases. Around such crossings, the Fock basis states can be strongly hybridized by the kinetic energy term. Even though these crossing points do not necessarily happen at the same U, their resonant regions, where the Fock basis hybridization is substantial, might be overlapping for sufficiently large electron hopping, leading to the delocalization of the whole spectrum. Importantly, the above argument becomes invalid if $V, U \gg 1$ (the weak hopping limit) and the resonant regimes are diluted, rendering MBL generic in the very weak hopping limit. A mathematically rigorous proof can be found in Refs. [9,10,38] for sufficiently large disorder, but it appears that this limit is reached already for $V \sim 4$–6 in Fig. 1. We cannot rule out the possibility that the critical MBL disorder depends somewhat on the system size [15].

Up to the intermediate region $U \sim \mathcal{O}(1)$, we find no qualitative differences between LR and SR results. However, this is no longer true for $U \gg 1$. Particularly, the strongly interacting phase with LR interaction is localized for all value of V for both models of disorder [see Figs. 1(b) and 1(d)]. This suggests that for LR interactions, the nature of the strongly interacting regime is disconnected from the noninteracting regime. In fact, the localization of all eigenstates when $U \to \infty$ is entirely driven by interactions, which is reminiscent of the mechanism of a Wigner crystal where the role of disorder is to only break the translational symmetry to pin down the Wigner crystal. The picture is completely different for SR interactions, as there apparently exist both localized and extended phases in the large-U limit [see Figs. 1(a) and 1(c)]. Obviously, disorder must play an important role in the phase transition for SR interactions. We emphasize that in Fig. 1 both A and AA models behave qualitatively similarly *vis-à-vis* SR and LR interaction dependence.

To understand the nature of various regions in the phase diagram, we perform a scaling analysis using the ansatz $\langle \mathcal{I} \rangle / (1 - \langle \mathcal{I} \rangle) \propto N_e^{\alpha}$ (or equivalently L^{α} as $L/N_e = 2$) [33] and find that the phase diagrams can be partitioned, depending on the value of α, into four zones: (i) marginal localized ($\alpha \sim 0$), (ii) reciprocal extended ($\alpha \sim -1$), (iii) relevant localized ($\alpha > 0$), and (iv) super-reciprocal extended ($\alpha < -1$). The results are presented in Fig. 2. One can think of the system size scaling process as gluing identical lattice segments, thus the scaling behavior depends on how the bulk "communicates" with the boundary. The disorder-driven localized phase obviously does not know about the boundary, leading to the marginal scaling ($\alpha = 0$). This is the standard MBL phase mostly discussed in the existing literature. On the other hand, for the extended or thermal phase, all electronic states can spread through the boundary to the extension lattice, suppressing the density fluctuations. Specifically, the density profile of a noninteracting many-body eigenstate is simply the sum of each constituent single-particle eigenstate, $n_{\mathrm{MB}}(i) = \sum_j n_{\beta_j}(i)$, where MB stands for "many-body," i labels the lattice sites, and β_j is the single-particle eigenstate index with $j = 1, \ldots, N_e$. Since all single-particle states are extended, we assume the form $n_{\beta_j}(i) = [1 + \phi_{\beta_j}(i)]/L$, where $\phi_{\beta_j}(i)$ is the oscillating part integrated to zero, analogous to the familiar Friedel oscillations. Because of the oscillating nature, $\sum_{i,j,k} \phi_{\beta_j}(i)\phi_{\beta_k}(i)$ must be subleading compared to L^3, thus

$$\sum_{i=1}^{L} n_{\mathrm{MB}}(i)^2 = \nu N_e + \mathcal{O}(1). \tag{4}$$

If we then replace $\sum_i^L |u_i^{(\alpha)}|^2$ in Eq. (3) by $\sum_i n_{\mathrm{MB}}(i)^2$, we find that $\langle \mathcal{I} \rangle \sim N_e^{-1}$, consistent with the observed reciprocal scaling $\alpha = -1$ if the extended phase is adiabatically connected to the single-particle picture.

However, the strongly interacting extended phase is more complicated. Numerical simulations show that this

phase has a stronger decreasing scaling behavior. Compared to its noninteracting counterpart, an interacting many-body eigenstate cannot be expressed as a product of single-particle wave functions. In fact, from the level statistics information, we know that the interacting extended phase follows the Gaussian orthogonal ensemble [33], i.e., no information of the original noninteracting product states can be retrieved from the interacting correlated states. As a result, the density fluctuations of the correlated extended eigenstates have higher order corrections (beside the homogeneous density distribution), leading to the super-reciprocal scaling exponent $\alpha < -1$. We do not rule out the possibility that $\langle \mathcal{I} \rangle$ might decay even faster than a power-law function of L.

Strong-U generic localization for LR interactions.—We now turn to the localized phase with relevant scaling. We emphasize that this phase only appears in the LR interaction case for very large U, unambiguously establishing it as a strongly correlated phenomenon. In fact, the change from the extended to the interaction-induced MBL at $U \sim 10$ looks like a sharp phase transition. The absence of this phase in the SR interaction case is also an interesting point and will be discussed later. In the limit $U \to \infty$, only Fock basis states having the same interaction energies can hybridize; for the LR interaction, such states can only be related by a global translation operator, i.e., states are related by shifting all occupied sites by the same amount. This immediately rules out a direct coupling through a single electron hopping, as this process only moves one occupied site at a time. In fact, we find that the lowest-order intraband coupling must scale as $(1/U)^{N_e}$, while the band splitting only scales polynomially $\sim N_e^{\gamma}$. This suppresses the intra-band resonance as the system size grows [33], resulting in the apparent relevant scaling behavior. This scaling clearly establishes that the localization is driven by the interaction. Similar to Wigner crystal, the LR characteristic of the interaction is decisive here [39]. On the other hand, for SR interactions, the scaling is marginal at large interactions, similar to the noninteracting case, suggesting a qualitatively different physics.

Symmetry between strong-U and weak-U limits for SR interactions.—Compared with LR interactions, the constraints imposed by the SR interaction do not completely exclude direct coupling terms between Fock basis states. We can identify an occupied or vacant site with an up or down spin, effectively mapping the electron model to the Heisenberg spin chain where, in the strong-U limit, dynamical processes must conserve the number of domain walls between one occupied and one vacant site. We consider two types of domain walls: a single domain wall (SW) with no other domain walls in its immediate vicinity, and double domain walls (DW) formed by two domain walls next to each other. Upon applying a single electron hopping to an SW, two additional domain walls are created, thus violating the conservation of domain wall number.

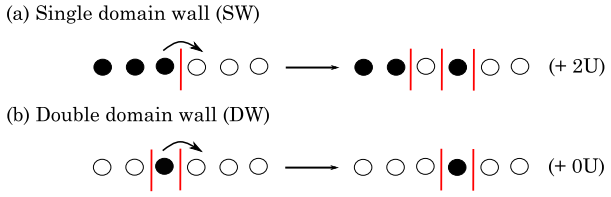

FIG. 3. (a) An immobile single domain wall and (b) an itinerant double domain wall.

Therefore, an SW is immobile when $U \to \infty$. On the other hand, the same operator moves the DW by one lattice constant without changing the total number of domain walls [see Figs. 3(a) and 3(b)] [40,41]. This is the intraband direct coupling that distinguishes between LR and SR cases when $U \to \infty$. A DW can thus propagate ballistically throughout the system like a free particle and is also subject to the disordered on-site potential. This simple picture suggests the symmetry between the $U \to 0$ and $U \to \infty$ limits for SR interactions [42].

The domain wall argument for SR interaction and the Fock state splitting for LR interaction that we presented above in the strongly interacting regime are actually forms of Hilbert space fragmentation [40,41,43,44]. The striking differences between the LR and SR cases arise because the coupling within each fragment is suppressed by U in the LR case while it is the original electron hopping in the SR case. In cold atom experiments, the hopping most likely occurs between nearest neighbors, while the interaction can assume a generic power-law function, e.g., r^{-3} for dipole-dipole interaction. Therefore, it is natural to ask whether our results in the strong interaction limit can be generalized to other forms of interactions. To this end, we now consider a more general form of interaction with $1 < \kappa < \infty$ in Eq. (2). The results presented in Fig. 4 indicate that the phase boundaries with different κ for $L = 14$ coincide with the SR case ($\kappa \to \infty$) until a critical value $U_c^{(\kappa)}$ then eventually reduce to zero, similar to the LR case ($\kappa = 1$). The SR behavior should dominate when $U_{i,i+1} > U_c > U_{i,i+N_e}$

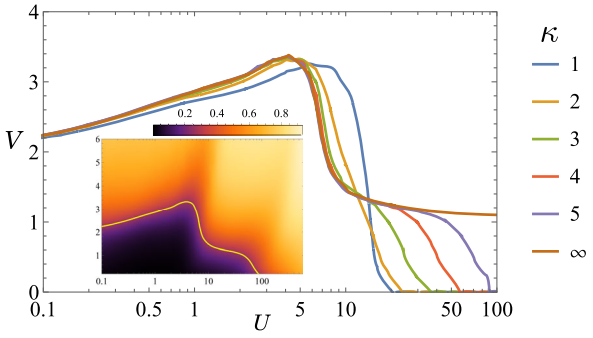

FIG. 4. Phase boundaries at different exponent κ defined by $\langle \mathcal{I} \rangle = 0.27$ for $L = 14$ so that they start at $V = 2$ for $U = 0$. The inset shows the mean IPR phase diagram for the exponent of 5 with the previously defined phase boundary.

while the LR behavior starts to manifest when $U_{i,i+N_e} > U_c$ with U_c being some threshold value. As a result, the critical value $\ln U_c^{(\kappa)} \sim \kappa$, which can be seen approximately in Fig. 4. Therefore, the two cases we study in depth in this work ($\kappa = 1$ and $\kappa = \infty$) can be thought of as two limiting cases between which lie other cases of generic interactions.

Conclusion.—We have presented the MBL quantum phase diagrams for SR and LR interactions in the random A and quasiperiodic AA models over a wide range of disorder and interaction strengths for interacting fermions in 1D tight-binding lattices. We establish that the interaction range plays a nontrivial role in MBL physics. Our findings include the generic MBL in both A and AA models when the disorder strength is $V > 4$–6 in lattice hopping units (and there is a generic symmetry between weak and strong interactions in the phase diagram for SR interactions), but MBL is generic for all disorder strengths in the strong LR interaction limit for both A and AA models. The phase diagram of a generic polynomially system should lie between these two limits. Experiments using cold atoms on optical lattices can verify our prediction of the generic interaction-driven MBL in LR interacting 1D systems.

This work is supported by Microsoft and Laboratory for Physical Sciences. This work is also generously supported by the High Performance Computing Center (HPCC) at the University of Maryland. X. L. also acknowledges support from the National Natural Science Foundation of China (Grant No. 11904305), the Research Grants Council of Hong Kong (Grants No. CityU 21304720 and No. CityU 11300421), as well as City University of Hong Kong (Project No. 9610428).

[1] R. Nandkishore and D. A. Huse, Annu. Rev. Condens. Matter Phys. **6**, 15 (2015).
[2] E. Altman and R. Vosk, Annu. Rev. Condens. Matter Phys. **6**, 383 (2015).
[3] D. A. Abanin, E. Altman, I. Bloch, and M. Serbyn, Rev. Mod. Phys. **91**, 021001 (2019).
[4] S. Gopalakrishnan and S. Parameswaran, Phys. Rep. **862**, 1 (2020).
[5] P. W. Anderson, Phys. Rev. **109**, 1492 (1958).
[6] J. M. Deutsch, Phys. Rev. A **43**, 2046 (1991).
[7] M. Srednicki, Phys. Rev. E **50**, 888 (1994).
[8] D. Basko, I. Aleiner, and B. Altshuler, Ann. Phys. (Amsterdam) **321**, 1126 (2006).
[9] J. Z. Imbrie, J. Stat. Phys. **163**, 998 (2016).
[10] J. Z. Imbrie, Phys. Rev. Lett. **117**, 027201 (2016).
[11] S. Aubry and G. André, Ann. Isr. Phys. Soc. **3**, 18 (1980).
[12] V. Oganesyan and D. A. Huse, Phys. Rev. B **75**, 155111 (2007).
[13] M. Žnidarič, T. Prosen, and P. Prelovšek, Phys. Rev. B **77**, 064426 (2008).
[14] A. Pal and D. A. Huse, Phys. Rev. B **82**, 174411 (2010).
[15] T. Devakul and R. R. P. Singh, Phys. Rev. Lett. **115**, 187201 (2015).
[16] X.-P. Li, S. Ganeshan, J. H. Pixley, and S. Das Sarma, Phys. Rev. Lett. **115**, 186601 (2015).
[17] Y.-T. Hsu, X. Li, D.-L. Deng, and S. Das Sarma, Phys. Rev. Lett. **121**, 245701 (2018).
[18] E. Khatami, M. Rigol, A. Relaño, and A. M. García-García, Phys. Rev. E **85**, 050102(R) (2012).
[19] R. Singh, R. Moessner, and D. Roy, Phys. Rev. B **95**, 094205 (2017).
[20] G. De Tomasi, Phys. Rev. B **99**, 054204 (2019).
[21] T. Botzung, D. Vodola, P. Naldesi, M. Müller, E. Ercolessi, and G. Pupillo, Phys. Rev. B **100**, 155136 (2019).
[22] N. Y. Yao, C. R. Laumann, S. Gopalakrishnan, M. Knap, M. Müller, E. A. Demler, and M. D. Lukin, Phys. Rev. Lett. **113**, 243002 (2014).
[23] A. L. Burin, Phys. Rev. B **92**, 104428 (2015).
[24] D. B. Gutman, I. V. Protopopov, A. L. Burin, I. V. Gornyi, R. A. Santos, and A. D. Mirlin, Phys. Rev. B **93**, 245427 (2016).
[25] Y.-L. Wu and S. Das Sarma, Phys. Rev. A **93**, 022332 (2016).
[26] R. M. Nandkishore and S. L. Sondhi, Phys. Rev. X **7**, 041021 (2017).
[27] A. A. Akhtar, R. M. Nandkishore, and S. L. Sondhi, Phys. Rev. B **98**, 115109 (2018).
[28] S. Roy and D. E. Logan, SciPost Phys. **7**, 042 (2019).
[29] M. Schreiber, S. S. Hodgman, P. Bordia, H. P. Luschen, M. H. Fischer, R. Vosk, E. Altman, U. Schneider, and I. Bloch, Science **349**, 842 (2015).
[30] H. P. Lüschen, P. Bordia, S. Scherg, F. Alet, E. Altman, U. Schneider, and I. Bloch, Phys. Rev. Lett. **119**, 260401 (2017).
[31] H. P. Lüschen, S. Scherg, T. Kohlert, M. Schreiber, P. Bordia, X. Li, S. Das Sarma, and I. Bloch, Phys. Rev. Lett. **120**, 160404 (2018).
[32] T. Kohlert, S. Scherg, X. Li, H. P. Lüschen, S. Das Sarma, I. Bloch, and M. Aidelsburger, Phys. Rev. Lett. **122**, 170403 (2019).
[33] See Supplemental Material at http://link.aps.org/supplemental/10.1103/PhysRevLett.128.146601, which includes Ref. [34], for thermodynamic extrapolation, level statistics, and domain wall description in the strongly interacting limit.
[34] Y. Y. Atas, E. Bogomolny, O. Giraud, and G. Roux, Phys. Rev. Lett. **110**, 084101 (2013).
[35] S. Nag and A. Garg, Phys. Rev. B **96**, 060203(R) (2017).
[36] S. Bera, H. Schomerus, F. Heidrich-Meisner, and J. H. Bardarson, Phys. Rev. Lett. **115**, 046603 (2015).
[37] S. Nag and A. Garg, Phys. Rev. B **99**, 224203 (2019).
[38] V. Mastropietro, Phys. Rev. Lett. **115**, 180401 (2015).
[39] D. D. Vu and S. Das Sarma, Phys. Rev. B **101**, 125113 (2020).
[40] G. De Tomasi, D. Hetterich, P. Sala, and F. Pollmann, Phys. Rev. B **100**, 214313 (2019).
[41] C. M. Langlett and S. Xu, Phys. Rev. B **103**, L220304 (2021).
[42] In particular, the IPR at fixed V as a function of U should demonstrate similar values for $U = 0$ and $U \to \infty$. We note that the domain wall argument is exact in the strong-U limit

and should be applicable nonperturbatively (in V). However, the symmetry is not quantitatively exact for small systems but should improve as the system size grows [33].

[43] P. Sala, T. Rakovszky, R. Verresen, M. Knap, and F. Pollmann, Phys. Rev. X **10**, 011047 (2020).
[44] V. Khemani, M. Hermele, and R. Nandkishore, Phys. Rev. B **101**, 174204 (2020).